Summary of the angular-momentum-dominated beam experiment (April and May 2004)

Y.-E Sun, University of Chicago
P. Piot, Fermi Lab.

July 13, 2004

Abstract

We present recent measurements of the angular momentum of a magnetized beam, i.e., a photo-emitted beam in the presence of a longitudinal magnetic field on the photocathode. The measurements are compared with numerical simulations.

1 Introduction

The 1-1/2 cell, 1.3 GHz RF photo-cathode gun at FNPL is surrounded by three solenoids (see Fig.1). Under nominal operation the two downstream solenoids (the "primary" and "secondary" solenoids) provide an external focusing to counteract the beam expansion due to space charge forces, while the first solenoid (refer to as "bucking solenoid") is used to zero the magnetic field at the photocathode location.
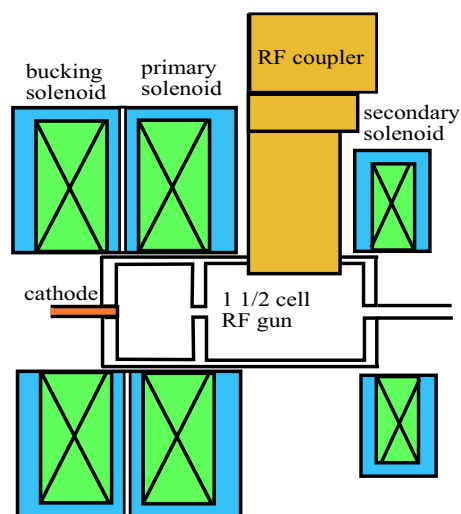

Figure 1: RF photo-cathode gun with three solenoids: bucking, primary, and secondary.

In order to produce an angular-momentum-dominated beam, for example, as needed for the production of a flat beam, a non-vanishing longitudinal magnetic field on the photocathode is required. The magnetic field on the cathode can be controlled by a proper tuning of the three solenoid currents. In the measurements reported hereafter, the bucking solenoid current is set to zero. The primary and secondary solenoid currents are adjusted in order to vary the magnetic field value on the photo-cathode while properly focusing the electron beam in order to enable its propagation up to the spectrometer location.

For the measurement reported in this Note, the total energy of the beam is measured to be approximately 15.8 ± 0.5 MeV downstream of the superconducting 9-cell TESLA type cavity. The charge per bunch is about 0.45 ± 0.05 nC. The measurements of angular momentum are performed downstream of the TESLA cavity: optical transition radiation (OTR) screens and multi-slits mask can be inserted at different locations as depicted in Fig. 2.
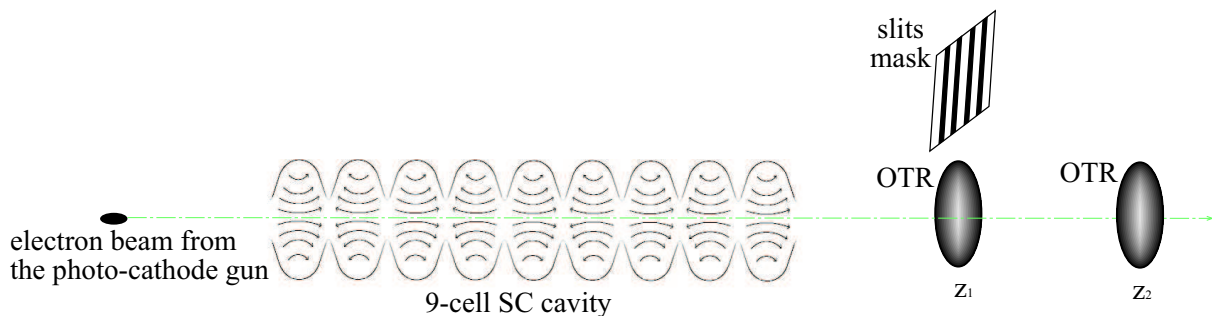

Figure 2: Overview of the experimental set-up for measurement of angular momentum. Slits can be inserted at location z_1 and OTR screens are available at both z_1 and z_2 locations.

2   Experimental Method

A first measurement of beam angular momentum as a function of the longitudinal magnetic field on the photocathode was reported in Reference [1]. Our goals in the present Note are: (1) to expand the aforementioned measurement to a wider range of the magnetic field on cathode (from $B_z \in [450, 700]$ Gauss in Ref. [1] to $B_z \in [200, 1100]$ Gauss) and (2) to detail the experimental method used. We use the same notation as used in Reference [1].

Due to the cylindrical symmetry of the system (laser, external magnetic and electron-magnetic fields), the canonical angular momentum is conserved. In cylindrical coordinates (r, ϕ, z), the canonical angular momentum L of an electron with radius r in a magnetostatic field $\vec{B}(r, z) = B_z(z)\vec{e}_z - \frac{1}{2}r\frac{d}{dz}B_z(z)\vec{e}_r$ (wherein $B_z(z)$ is the longitudinal magnetic field) is given by[2]:

$$L = \gamma m r^2 \dot{\phi} + \frac{1}{2}eB_z r^2,$$

(1)

where γ is the Lorentz factor, m and e are respectively the electron rest mass and charge, $\dot{\phi}$ the time derivative of ϕ, and $\vec{e}_z$ and $\vec{e}_r$ are the longitudinal and radial unit vectors. Here $B_z \doteq B_z(0)$ is the longitudinal magnetic field on the photocathode (located a $z = 0$); it is assumed to be r-independent.

We are interested in measuring the canonical angular momentum at the photocathode and study its conversion into mechanical angular momentum downstream of the TESLA cavity.

To estimate the canonical angular momentum at the photocathode location, we simply remark that the first term of Eq.1 vanishes at the photocathode location since $\dot{\phi} = 0$. The canonical angular momentum averaged over the beam distribution $\langle L \rangle$ is then:

$$\langle L \rangle = \frac{1}{2} e B_z \langle r^2 \rangle = e B_z \sigma_c^2, \tag{2}$$

where the value for B_z may be obtained from POISSON [3] simulations given the currents in the solenoids, and $\sigma_c = \sqrt{\langle r^2 \rangle / 2}$ is the horizontal or vertical rms beam size on the photocathode. Thus from a measurement of the beam spot size on the photocathode and a calculation of the expected magnetic field on the photocathode given the solenoid currents, we have a direct estimate of the averaged canonical angular momentum.
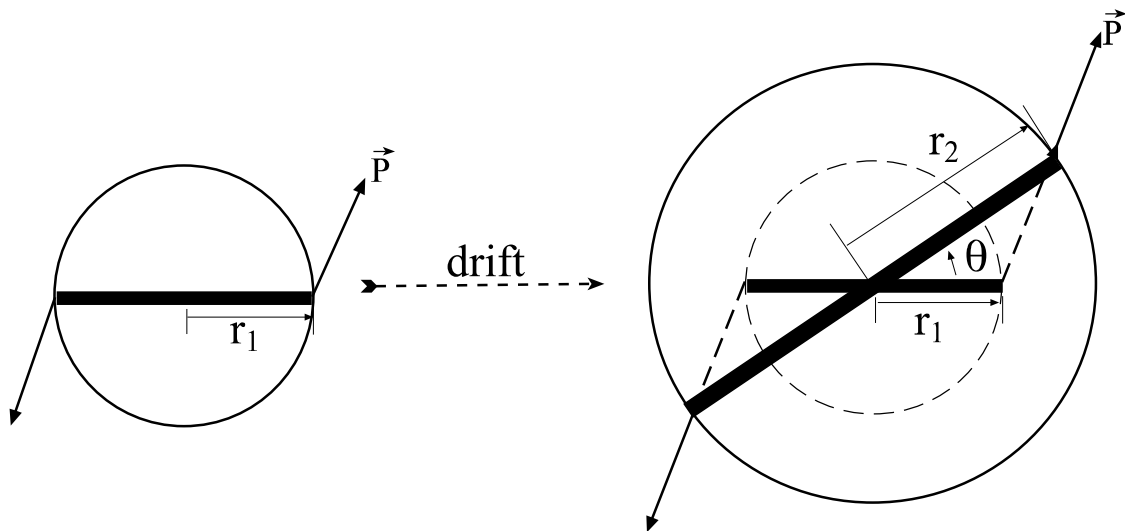

Figure 3: Beam with canonical angular momentum-induced sheering while drifting. The dark narrow rectangular can be a slit inserted into the beam line in order to measure the sheering angle.

In the region where $B_z(z) = 0$, e.g. downstream of the TESLA cavity, the second term of Eq.1 vanishes and the canonical angular momentum equals to the mechanical angular momentum. To measure the mechanical angular momentum, let's consider an electron, in a magnetic field-free region, at longitudinal location z_1 with transverse radial vector

3

$\vec{r}_1 = r_1 \vec{e}_x$. After propagation through a drift space, the electron reaches $\vec{r}_2$ at location z_2. Let $\theta \doteq \angle(\vec{r}_1, \vec{r}_2)$ be the angle between the two aforementioned radial vectors (henceforth referred to as "sheering angle"). It can be experimentally measured by inserting at location z_1 a multi-slit masks and by measuring the corresponding rotation angle of the beamlets at the location z_2 (this is pictorially illustrated in Fig. 3).

The mechanical angular momentum of the electron, $\vec{L}$, is given by:

$$\vec{L} = r_1 \vec{e}_x \times \vec{P} = r_1 P_y \vec{e}_x \times \vec{e}_y. \tag{3}$$

Let $y' \doteq \frac{dy}{dz} = \frac{P_y}{P_z}$, where P_y and P_z are the vertical and longitudinal components of the momentum, y' is a constant in a drift space (for an emittance-dominated beam). The change in y coordinate, Δy, can be calculated via:

$$\Delta y = \int_0^D y' dz = y' D.$$

On the other hand, from Fig. 3, we have $\Delta y = r_2 \sin\theta$, so that $y' = r_2 \sin\theta / D$. Hence Eq. 3 can be re-written in the convenient form:

$$\vec{L} = r_1 P_z y' \vec{e}_z = P_z \frac{r_1 r_2 \sin\theta}{D} \vec{e}_z. \tag{4}$$

Let the rms beam radii be σ_1^r and σ_2^r at z_1 and z_2, respectively. For a laminar beam, the canonical angular momentum averaged over the beam distribution can then be calculated via:

$$\langle L \rangle = P_z \frac{\sigma_1^r \sigma_2^r \sin\theta}{D}. \tag{5}$$

Finally, for a cylindrically symmetric beam, the rms beam size on horizontal and vertical axes, σ^x and σ^y, are related to the rms beam radius by: $\sigma^x = \sigma^y = \sigma^r / \sqrt{2}$. Thus Eq. 5 can be written as:

$$\langle L \rangle = 2 P_z \frac{\sigma_1 \sigma_2 \sin\theta}{D}, \tag{6}$$

where $\sigma_1 \doteq \sigma_1^x = \sigma_1^y$, $\sigma_2 \doteq \sigma_2^x = \sigma_2^y$.

Thus a measurement of rms beam size at location z_1 and z_2 along with the corresponding sheering angle, as the beam propagates from z_1 to z_2, provide the required information for calculating the beam mechanical angular momentum.

3   Experimental Results

The magnetic field on the cathode was varied (see Table 1) by properly adjusting the solenoids currents. The laser transverse spot size on the cathode was held constant and measured to be $\sigma_x \simeq \sigma_y \simeq 0.98$ mm on the "virtual photocathode" (an optical image of the photocathode plane observed on a piece of fluorescent paper via a calibrated CCD camera). This measurement together with the estimated value of the longitudinal magnetic field on the photocathode can be plugged in Eq. 2 to yield the canonical angular momentum.

solenoid current [A]		magnetic field on cathode [Gauss]	
primary	secondary	POISSON	linear combination
40	295	229	222
60	295	325	313
80	195	421	404
100	295	517	495
120	295	613	586
140	255	702	672
160	255	794	763
180	220	877	850
200	180	959	935
220	80	1031	1013
240	0	1105	1094

Table 1: Magnetic field on the photo-cathode for different primary and secondary solenoid currents settings. The bucking solenoid current is set to zero. The column "POISSON" are simulation results by putting the solenoid currents directly into the simulation, while the "linear combination" column are results from the following linear equation: $B_z[\text{Gauss}] = 774.54 \times \frac{I_p[\text{A}]}{170} + 9.38 \times \frac{I_s[\text{A}]}{70}$, where I_p and I_s are the primary and secondary solenoid current, respectively.

To measure the mechanical angular momentum downstream of the TESLA cavity, two OTR stations were used, as depicted in Fig. 2. At location $z_1 = 3.678$ m, both an OTR screen (for beam spot size measurements), and multi-slit mask (for sheering angle measurement) can be inserted. After a drift of distance 1.375 meter, another OTR viewer is available (at $z_2 = 5.053$m). The measurement consists of the following sequence: (1) measure the beam rms size at location z_1 and z_2, and (2) insert the vertical muli-slit mast at location z_1 and measure the sheering angle by observing the slits image at location z_2. An example of the such measurement sequence is depicted in Fig. 4. The measurements of the rms beam sizes at z_1 and z_2 along with the corresponding sheering angle θ and the estimated mechanical angular momentum from Eq. 6 are summarized in Fig. 5. In the latter Figure, the bottom right plot compares the averaged mechanical angular momentum with canonical angular momentum and agreement between these two quantities is at the 10 % level.

4   Numerical benchmarking of the experiment method

Although the measurements reported in the previous Section tend to indicate the canonical angular momentum at the photocathode is converted into mechanical angular momentum (as measured downstream of the TESLA cavity), the agreement is at the 10 % level. It is therefore interesting, for completeness, to investigate via simulations the expected performance of measurement technique used in this Note. We have used the program ASTRA to simulate the beam dynamics: the simulations are set-up to mimic the experimental condi-

tions (photocathode laser, RF amplitudes, phases, etc...).

We first compared in Fig. 6 the canonical angular momentum of the beam at the photocathode (computed as $\sum_{i=1}^{N_{mac}} \frac{1}{2}eBr_i^2$ where the sum is performed over the macroparticles used in the simulation, and N_{mac} is the number of macroparticles) with the mechanical angular momentum downstream of the TESLA cavity (computed as $\sum_{i=1}^{N_{mac}} \frac{1}{p_{z,i}}(x_i p_{y,i} - y_i p_{x,i})$). The agreement is excellent.

Finally the simulations of the measurement technique for the various case of solenoid settings considered in the experiment are summarized in Fig. 7 (this Figure should be compared with Figure 5). The beam spot sizes at z_1 and z_2 were directly evaluated after tracking the beam with ASTRA. The phase space produced by ASTRA at z_1 was used to simulate the multi-slit mask, and the so-generated beamlets at z_1 were tracked up to z_2 using linear transport matrix. The beam sizes at z_2 generated by tracking the phase space distribution at z_1 using linear optics were checked to agree with ASTRA simulation. The retrieved values for the mechanical angular momentum, obtained after simulation of the experiment, agree within 10-20 % with the canonical angular momentum computed at the photocathode.

5 Conclusion

In this Note the experimental method we used to measure the beam angular momentum is explained in detail. ASTRA simulations which mimic the experimental technique are performed and checked against experimental results. We conclude that when applied, the aforementioned technique gives measured mechanical angular momentum values that are within theoretically expected values at a ± 10 % level for a wide range of magnetic field on cathode([200, 1100] Gauss).

References

[1] Y. Sun, *et al.*,"Angular Momentum Measurement of the FNPL Electron Beam", *Proceedings of 2003 Particle Accelerator Conference, Portland, OR*, 2682-2684, (2003).

[2] M. Reiser, "Theory and Design of Charged Particle Beams", John Willey & Sons, INC., 1994, pp. 33-35.

[3] J. H. Billen and L. M. Young, "POISSON/SUPERFISH on PC Compatibles," *Proceedings of the 1993 Particle Accelerator Conference, Washington DC*, 790-792 (1993)

[4] K. Flöttmann, "ASTRA: A Space Charge Tracking Algorithm", user manual available at `http://www.desy.de/∼mpyflo/Astra_dokumentation`.
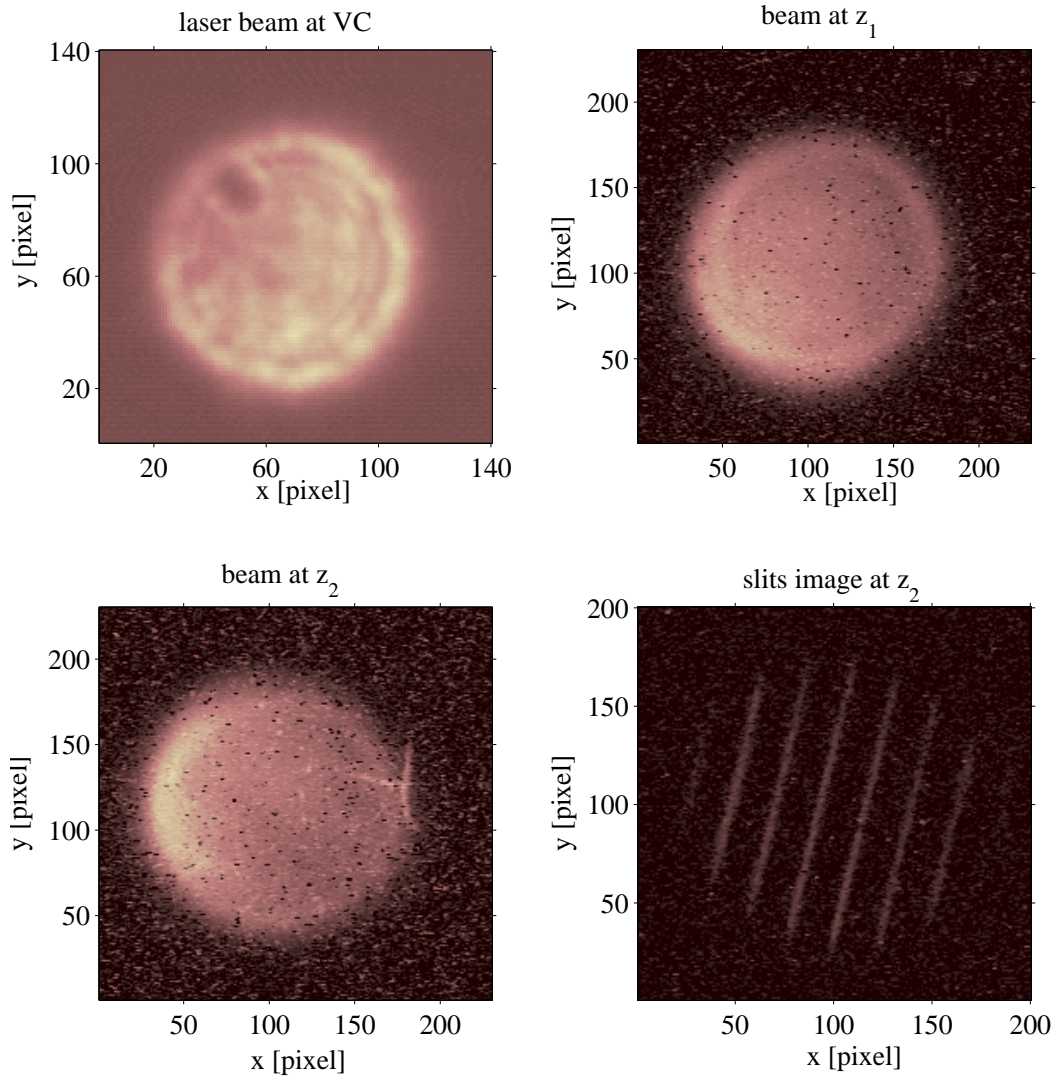
Figure 4: Example of experimental measurements sequence needed to calculate the canonical angular momentum at the photocathode and mechanical angular momentum downstream of the TESLA cavity.
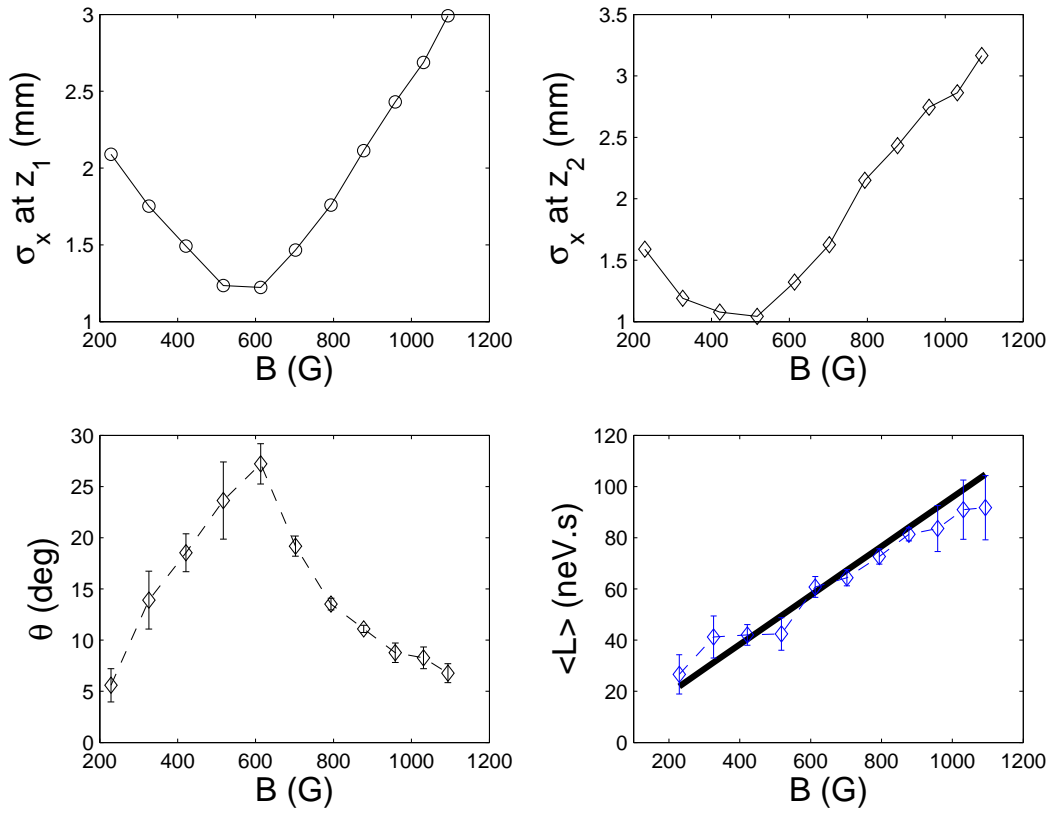
Figure 5: Experimental data: rms beam sizes at locations z_1 and z_2 (top plots), rotation angle at z_2 from slits inserted at z_1 (bottom left plot) and comparison of the deduced mechanical angular momentum with expected canonical angular momentum at the photocathode (bold line).
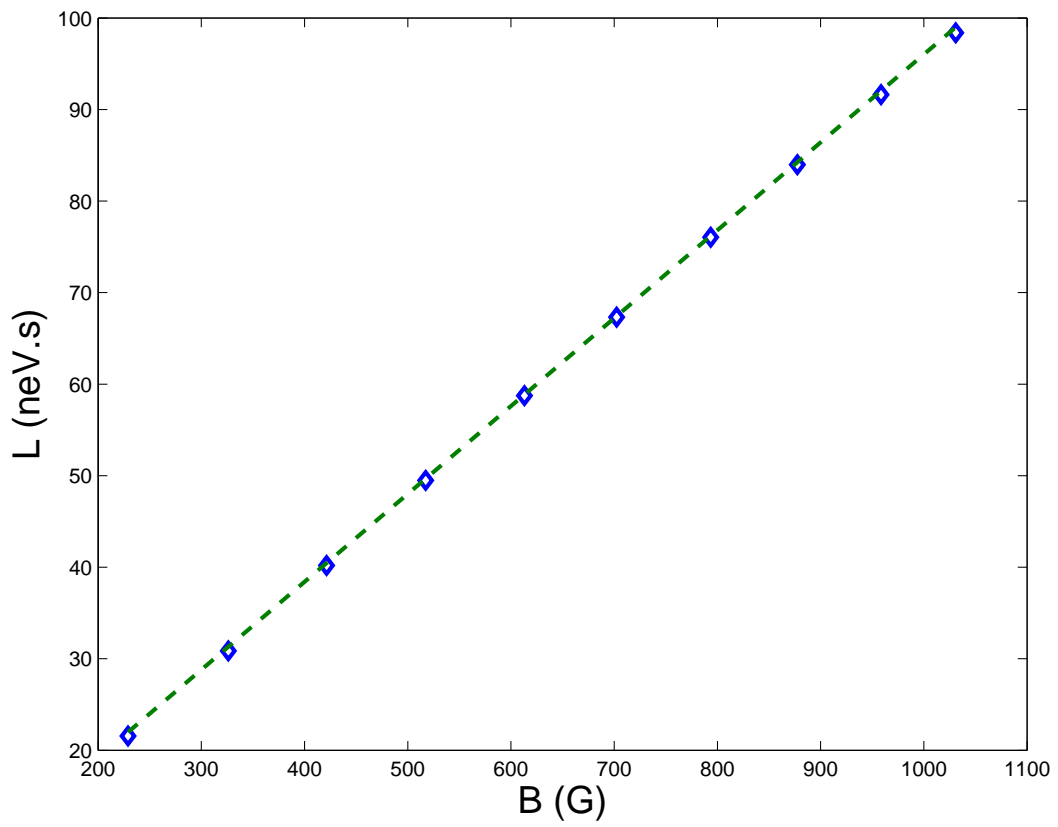
Figure 6: Comparison of the canonical angular momentum computed at the photocathode with the electron beam mechanical angular momentum calculated downstream of the TESLA cavity. The tracking from the photocathode to downstream of the TESLA cavity have been performed using ASTRA including space charge effects.
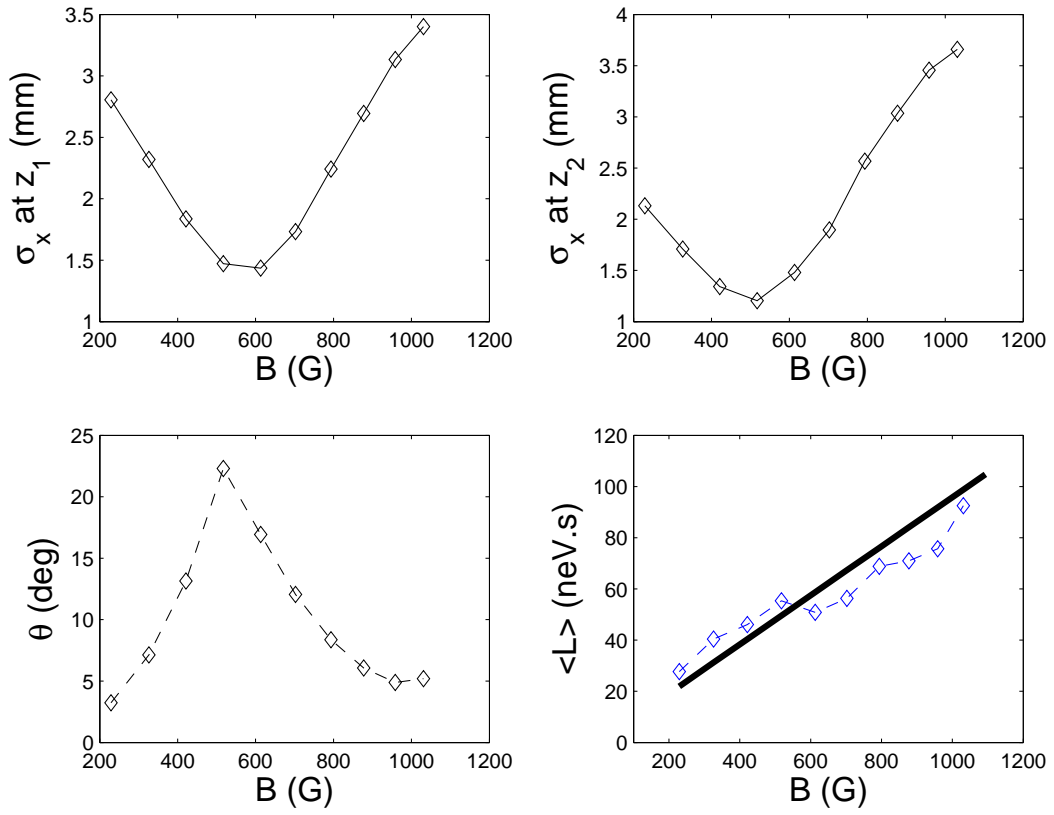
Figure 7: Simulation of the experiment: rms beam sizes at locations z_1 and z_2 (top plots), rotation angle at z_2 from slits inserted at z_1 (bottom left plot) and comparison of the deduced mechanical angular momentum with expected canonical angular momentum at the photocathode (bold line).